

**VACUOLAR DEGRADATION OF RAT LIVER CYP2B1 IN *SACCHAROMYCES
CEREVISIAE*: FURTHER VALIDATION OF THE YEAST MODEL AND STRUCTURAL
IMPLICATIONS FOR THE DEGRADATION OF MAMMALIAN ENDOPLASMIC
RETICULUM P450 PROTEINS**

Mingxiang Liao, Victor A. Zgoda¹, Bernard P. Murray² and Maria Almira Correia^b

Departments of Cellular and Molecular Pharmacology, Pharmaceutical Chemistry, and
Biopharmaceutical Sciences and the Liver Center, University of California, San Francisco,
California 94143

[Please Note: The work was carried out while Drs. Murray and Zgoda were still at the University
of California, San Francisco. Hence the footnotes to their current addresses.]

a). **RUNNING TITLE: DEGRADATION OF CYP2B1 and CYP2B1-3A4CT IN *S. CEREVISIAE***

b). #Corresponding Author:

M. A. Correia

Dept. of Cellular and Molecular Pharmacology,
Box 0450
University of California
San Francisco, CA 94143-0450
415-476-3992 (TEL)
415-502-2467 (FAX)
e-mail: mariac@itsa.ucsf.edu

c). Number of text pages: 28
Number of tables: 3
Number of figures: 9
Number of References: 40
Abstract: 250 words
Introduction: 744 words
Discussion: 1422 words

d). Abbreviations used: Cytochromes P450 (P450s; CYPs); Degradation in ER (DER); endoplasmic reticulum (ER); ER-associated degradation (ERAD); 3-hydroxy-3-methylglutaryl-CoA reductase (HMGR); HMGR Degradation (HRD); phenobarbital (PB); ubiquitin (Ub); Ub-Conjugation (UBC); Ub-conjugating enzyme (Ubc).

ABSTRACT

Mammalian hepatic cytochromes P450 (P450s) are endoplasmic reticulum (ER)-anchored hemoproteins with highly variable half-lives. CYP3A4, the dominant human liver drug-metabolizing enzyme, and its rat liver orthologs undergo ubiquitin (Ub)-dependent 26S proteasomal degradation after suicide inactivation or after heterologous expression in *S. cerevisiae*. In contrast, rat liver CYP2C11 is degraded by the vacuolar “lysosomal” pathway when similarly expressed in yeast. The structural determinants that commit P450s to proteasomal or lysosomal degradation are unknown. To further validate *S. cerevisiae* as a model for exploring mammalian P450 turnover, the degradation of phenobarbital-inducible liver CYP2B1, an enzyme reportedly degraded via the rat hepatic autophagic-lysosomal pathway, was examined in a yeast strain (*pep4Δ*) deficient in vacuolar degradation and its isogenic wild type control (*PEP4*). Although CYP2B1 was equivalently expressed in both strains during early logarithmic growth, its degradation was retarded in *pep4Δ*-strain, remaining at a level five-fold higher than that in *PEP4*-yeast when monitored at the stationary phase. No comparable CYP2B1 stabilization was detected in yeast genetically deficient in the ER Ub-conjugating enzyme Ubc6p or Ubc7p, or defective in 19S proteasomal subunit Hrd2p. Thus as in the rat liver, CYP2B1 is a target of vacuolar/lysosomal, rather than proteasomal degradation in yeast, thereby further validating this model for mammalian P450 turnover. Intriguingly, a chimeric protein CYP2B1-3A4CT, with the CYP3A4 C-terminal heptapeptide grafted onto CYP2B1 C-terminus, was proteasomally degraded after similar expression. Such diversion of CYP2B1 from its predominantly vacuolar degradation suggests that the CYP3A4-heptapeptide could either actively signal its proteasomal degradation or block its vacuolar proteolysis.

INTRODUCTION

Mammalian liver cytochromes P450 (P450s) are monotopic, endoplasmic-reticulum (ER)-anchored proteins engaged in the biotransformation of various endo- and xenobiotics. They are a superfamily of constitutive and inducible hemoproteins whose hepatic content, diversity and/or function can be modulated by their substrates through altered synthesis and/or turnover³ (Correia, 1991, 2003 *and references therein*). Studies of individual isoforms reveal that P450 protein turnover is highly variable ($t_{1/2} \approx 7-37$ h) but the basis for this heterogeneity has yet to be elucidated. A major deterrent to the characterization of P450 turnover is the lack of a suitable experimental model wherein this physiological process can be faithfully reproduced. For instance, the ER-bound P450s phenobarbital (PB)-inducible CYP2B1 and ethanol-/acetone-complexed CYP2E1 exhibit protein half-lives of ≈ 37 h and are degraded by the autophagolysosomal pathway in the rat liver (Masaki et al., 1987; Ronis et al., 1989, 1991)⁴. In contrast, CYP2B1 and CYP2E1 stably expressed in HeLa cells exhibit considerably shorter half-lives ($t_{1/2} \approx 8.7$ and 3.7 h, respectively), and are degraded in an ubiquitin (Ub)-*independent* process, blocked by specific proteasomal but not lysosomal inhibitors (Huan et al., 2004). The basis for this accelerated P450 protein turnover and altered degradation route is unclear.

In the search for a model for the mechanistic characterization of mammalian liver P450 turnover, we have employed *Saccharomyces cerevisiae*. This model has been used to characterize the ER-associated degradation (ERAD) of several integral and luminal proteins (Hampton, 2002a, 2002b; Kostova and Wolf, 2003), most notably, the polytopic ER protein Hmg2p [the yeast form of 3-hydroxy-3-methylglutaryl-CoA reductase (HMGR); Fig. 1], and CPY* (a misfolded carboxypeptidase mutant retained in the ER-lumen). Through genetic screens UBC (**Ub**-**C**onjugation), HRD (**H**MGR **D**egradation) and DER (**D**egradation in **ER**) genes have been identified that are critical for Hmg2p and CPY* ERAD (Hampton, 2002a, 2002b; Kostova

and Wolf, 2003). This UBC/HRD/DER machinery includes: (i) ER-associated Ub-conjugating enzymes (Ubc1p, Ubc6p and Ubc7p), (ii) Hrd2p, a 19S subunit that is essential for 26S proteasome function, (iii) Hrd1p/Hrd3p complex, an ER-associated Ub-ligase, and (iv) Cdc48p-Ufd1p-Hrd4p complex responsible for the recognition of polyubiquitinated ER proteins, their ER dislocation, and subsequent delivery to the 26S proteasome. Mammalian homologs of the yeast HRD/DER machinery attest to the high evolutionary conservation of the ERAD process (Hampton, 2002a, 2002b; Kostova and Wolf, 2003).

Similar analyses have also identified the *PEP4* gene as important in determining protein turnover. This gene encodes vacuolar proteinase A (YscA), a critical enzyme in the posttranslational processing and functional maturation of vacuolar proteases. The yeast vacuole is analogous to the mammalian lysosome as a degradation site of various proteins, including cytosolic, vacuolar and integral membrane proteins (Wolf, 2004). Yeast strains with *PEP4* gene disruptions (*pep4Δ*) are defective in vacuolar proteinase function and provide a diagnostic tool for probing vacuole-dependent degradation.

Because of the high conservation between yeast and mammalian degradation pathways, and the availability of validated genetic *S. cerevisiae* strains with defined defects in vacuolar and Ub-dependent proteasomal degradation, the yeast model was used to characterize the degradation of CYP3A4, the dominant human liver P450 (Murray and Correia, 2001). These findings revealed that CYP3A4 degradation in *S. cerevisiae* required a fully functional Ub-dependent proteasomal system, but was independent of the *PEP4*-dependent vacuolar pathway. Thus, in common with Hmg2p ERAD, CYP3A4 ERAD involved Ubc7p and Hrd2p, but unlike Hmg2p ERAD, CYP3A4 ERAD was independent of Hrd1p/Hrd3p Ub-ligase complex. In contrast, similar studies of rat CYP2C11 in *S. cerevisiae*, identified the *PEP4* vacuolar pathway rather than the *HRD*-dependent pathway as the principal degradation route for this integral ER

protein (Murray et al., 2002). This differential degradation of these heterologously expressed mammalian P450s reveals that although they are both “alien” to *S. cerevisiae* they are not both targeted for rapid proteolytic clearance, as would be the case for misfolded proteins. This finding also infers the existence of intrinsic structural determinants for the differential proteolytic targeting of P450s. To further assess the validity of this model for mammalian P450 turnover analyses, the degradation of CYP2B1, normally a substrate of the autophagic-lysosomal pathway in the rat liver (Masaki et al., 1987; Roberts, 1997; Ronis et al., 1991) was examined in *S. cerevisiae*. Furthermore, in an initial attempt to identify the structural determinant(s) that commits this P450 to a specific proteolytic pathway, the degradation of a CYP2B1-3A4 chimera, consisting of the CYP3A4 C-terminal heptapeptide fused to the CYP2B1 C-terminus, was also examined in *S. cerevisiae*. These findings and the possible role of the P450 C-terminus in the differential proteolytic targeting of these proteins are discussed.

MATERIALS and METHODS

Materials: Media for yeast growth were purchased from Clontech (Palo Alto, CA). Cloning reagents such as restriction enzymes, ligases and Vent polymerase were obtained from New England BioLabs (Beverly, MA). pGEM-T Easy Vector was from Promega (Madison, WI). Rabbit polyclonal IgGs were raised commercially against CYP2B1 enzyme (purified from PB-pretreated rat livers) and purified by Protein A-Sepharose affinity chromatography.

Yeast Strains: The strains used, grouped as isogenic sets, are listed in Table 1. The methods for their construction have been described previously (Hampton and Rine, 1994; Hampton, 1996; Wilhovsky et al., 2000).

Plasmids: (i) CYP2B1 Expression Vectors: The rat CYP2B1 cDNA was amplified by PCR (with pSW1 encoding the full-length rat CYP2B1 as the template) and cloned into pYES2/CT (URA-marked, under the control of the yeast GAL1 promoter) and pYcDE-2 (TRP-marked 2 μ plasmid under the control of the yeast ADH1 promoter) to yield pYES2-2B1 and pYcDE-2B1, respectively. pKKCYP2B1(His)₄ encoding a full length CYP2B1 protein with a Glu₂ → Ala mutation for codon optimization (John et al., 1994), was a generous gift from Prof. J. R. Halpert, Univ. of Texas, Galveston.

(ii) CYP2B1-3A4CT Expression Vectors: Using PCR, with pYES2-2B1 as the template, the 21 C-terminal nucleotides from the CYP3A4 coding sequence were incorporated at the C-terminus of the CYP2B1 cDNA to generate CYP2B1-3A4CT. The CYP2B1-3A4CT fusion was inserted into pYcDE-2 and pYES2/ADH (modified from pYES2/CT, URA-marked, under the control of the yeast ADH1 promoter instead of the GAL1 promoter) to yield pYcDE/2B1-3A4CT and pYES2-ADH/2B1-3A4CT, respectively. The following primers were used for CYP2B1-3A4CT construction: PCR forward primer, 5'-CGT CGA CCC GTG GTT ACA CCA GGA CCAT-3'; PCR

reverse primer, 5'-ATC AGG CTC CAC TTA CGG TGC CAT CCC GAG CTG AGA AGC AGA TCT GGT ACG TTG GAG-3'. pKK2B1-3A4CT(His)₄ was similarly constructed by inserting the nucleotides coding for the seven C-terminal CYP3A4 residues in-frame into pKK2B1wt(His)₄ between those encoding the extreme C-terminus of the CYP2B1 cDNA and the start of the His₄-tag by conventional site-directed mutagenesis techniques.

Yeast Cell Transformation: This was carried out according to the detailed protocol (Clontech PT3024). The conditions for the growth of the cultures have been described previously (Murray and Correia, 2001; Murray et al., 2002). Briefly, yeast strains transformed with CYP2B1 expression vector or the corresponding empty vector were grown at 30°C in SD medium with appropriate supplements. Cells were harvested at an early culture stage during the logarithmic growth phase of the culture (OD of ≈1.0 at 600 nm), or at a late stage (after "stationary chase" generally 20 to 24 h after reaching an OD of 0.5 at 600 nm).

Bacterial Expression and Functional Reconstitution of CYP2B1 and CYP2B1-3A4CT: CYP2B1 and CYP2B1-3A4CT were expressed in *E. coli* DH5α using the expression vectors pKK2B1wt(His)₄ and pKK2B1-3A4CT(His)₄, respectively, as described previously (Wang et al., 1998). The enzymes were partially purified from CHAPS-solubilized bacterial membranes by Ni²⁺-NTA affinity chromatography, followed by extensive dialysis of the imidazole (200 mM)-eluted P450 proteins. The enzymes were reconstituted with P450 reductase and their testosterone 16β-hydroxylase activity was monitored as a CYP2B1 functional probe as described previously (He et al., 1996).

Microsomal Preparation: Yeast microsomal fractions were prepared as described previously (Murray and Correia, 2001), except that they were enriched by removal of the other cellular

contaminants by a differential sucrose gradient ultracentrifugation step. Briefly, spheroplasts were suspended in 2 volumes of 50 mM Tris-HCl buffer, pH 7.5, containing 10 mM MgSO₄, 0.1 mM EDTA, 10 mM K-acetate, 1 mM DTT, and protease inhibitors (1 mM PMSF, 0.1 mM AEBSF, 5 mg/L leupeptin, 10 mg/L aprotinin, 1 μM bestatin, 1 μM E-64, and 1 mg/L pepstatin). The spheroplast suspension was sonicated and then sedimented at 15,000g at 4°C for 15 min. The 15,000g supernatant was then carefully overlaid over 20% sucrose, and centrifuged at 100,000g at 4°C for 2 h. The sucrose layer containing light microsomes and the microsomal pellet were resuspended in 15 ml of 0.1 M K-phosphate buffer, pH 7.4, containing 1 mM DTT and 0.1 mM EDTA and resedimented at 100,000g at 4°C for 1 h and “washed” as described previously (Murray and Correia, 2000). The microsomal pellet was overlaid with K-phosphate buffer, pH 7.4, containing 1 mM DTT, 0.1 mM EDTA and 20% (v/v) glycerol and stored at -80°C until used.

CYP2B1 Immunoblotting Analyses: Microsomal protein (10 μg) from early and late stage cultures was used in these analyses. The protein content was normalized after methanol/H₂SO₄-precipitation and acetone-washes of yeast microsomes to eliminate interference in the protein assay of variable amounts of adventitious chromophoric material. Microsomal CYP2B1 protein content was assayed by western immunoblotting analyses similar to those described previously (Murray and Correia, 2001), except that the electroblotted membranes were exposed overnight to rabbit polyclonal anti-rat CYP2B1 IgGs (1:7000, v:v) as the primary antibody. The CYP2B1 immunoblots were densitometrically quantitated as described previously (Murray and Correia, 2001; Murray et al., 2002). The relative CYP2B1 content at the late stages of culture was expressed as a percentage of the corresponding CYP2B1 content (100%) at the early stage. Values depicted represent the mean ± SD of at the least 3 - 5 individual experiments.

Mol #9654

Slot-blotting Analyses: The phenotype of the yeast strain used was validated by following the degradation of Myc-tagged Hmg2p in parallel by immunoblotting analyses as described (Murray and Correia, 2001), except that polyclonal anti-Myc IgGs were used.

Statistical Analyses: Analyses were performed by Student's t-test using Microsoft Excel. A value of $p < 0.05$ was considered statistically significant.

RESULTS:

Independence of CYP2B1 degradation from the normal *UBC/HRD* ERAD-machinery: In preliminary experiments, we confirmed that only yeast strains transformed with the CYP2B1 expression vectors, but not the empty vectors, were capable of expressing CYP2B1. The authenticity of the *UBC* and *HRD* gene functionality (or lack thereof), of these strains was also verified by examining the degradation of chromosomally integrated 6Myc-HMG2 by immunoblotting analyses, essentially as described previously (Murray and Correia, 2001; Murray et al., 2002; *Data not shown*). Of the available protein turnover methods in yeast (Hampton et al., 1996; Kornitzer, 2002), the “*stationary chase*” was found to be the most suitable method for monitoring the degradation of the relatively long-lived protein, CYP2B1. The specific goal was to *qualitatively* define the particular *route* of degradation and the *roles* of certain enzymes/proteins in that pathway through the use of specific HRD, UBC or PEP4 deletion/defective mutants and corresponding wild type isogenic *S. cerevisiae* strains, rather than to quantitatively assess the relative *rates* of P450 degradation through these yeast proteolytic pathways. To validate the “*stationary chase*” method for assessing P450 degradation, CYP2B1 turnover was also monitored by the pulse-chase technique. ³⁵S-methionine was added to the RHY1166 culture in a methionine/cysteine-free medium at a culture density of ≈ 1.0 (\approx early stage) and chased with cold methionine/cysteine after 1 h. Labeled CYP2B1 was assayed by fluorography of immunoprecipitates of yeast lysates ($n = 3$ separate experiments). After 21 h (\approx late stage) we found that $43 \pm 5\%$ of the labeled CYP2B1 remained (i.e. loss of $\approx 57\%$ of early stage content) and this corresponded very nicely to the value determined by the “*stationary chase*” method ($38 \pm 10\%$ remaining at 21 h, or a loss of $\approx 62\%$). However unlike the total microsomal CYP2B1 content which continued to decline, the radiolabeled CYP2B1 content reached a steady level at around this time (as noted by Kornitzer, 2002). Since the stationary chase was performed with microsomal preparations, whereas the immunoprecipitation analyses were with yeast lysates, it is possible that the immunoprecipitated

CYP2B1 content at later (> 21 h) times reflects both its microsomal as well as non-microsomal pools (possibly sequestered within the autophagic-vacuoles).

The relative importance of either ER-associated Ub-conjugating enzyme Ubc6p or Ubc7p, or both these enzymes in CYP2B1 degradation was examined by pYcDE-2B1 expression in *ubc6Δ*, *ubc7Δ* and *ubc6Δ/ubc7Δ* yeast strains, deficient in either or both enzymes. During the stationary phase of culture⁵ there were no statistically significant differences in CYP2B1 stabilization in any of these strains relative to that in the corresponding *wt S. cerevisiae* strain (Fig. 2). These findings thus indicated that CYP2B1 degradation was independent of either of the two Ub-conjugating enzymes previously shown to be involved in ERAD.

Similar expression analyses in *wt* and *hrd2-1*, *hrd1Δ* and *hrd3Δ S. cerevisiae* strains revealed comparable CYP2B1 degradation and thus no CYP2B1 stabilization in any of the *hrd*-defective/deficient strains relative to the corresponding *wt* strain when monitored at the stationary phase of culture (Fig. 3). These findings indicated that CYP2B1 degradation was independent of Hrd2p, and thus of the 26S proteasome, a feature in common with the degradation of CYP2C11 but not with that of CYP3A4. Furthermore, in common with the degradation of both CYP2C11 and CYP3A4, the degradation of CYP2B1 was also independent of the Hrd1p/Hrd3p Ub-ligase complex responsible for Hmg2p ubiquitination in *S. cerevisiae*.

PEP4-gene dependence of CYP2B1 degradation: pYES2-2B1 expression analyses revealed a marked (\approx 5-fold) relative CYP2B1 stabilization in the *pep4Δ* strain compared to the content in the *wt (PEP4)* strain at the stationary phase of culture (Fig. 4). This level of retardation in degradation was thus much more pronounced than the two-fold stabilization of CYP2C11 previously observed in this same strain (Murray et al., 2002), thereby revealing the critical

importance of the vacuolar pathway for CYP2B1 degradation in yeast. These findings are consistent with the lysosomal degradation of CYP2B1 documented in the rat liver and thus provide further validation of this yeast model for the characterization of mammalian P450 turnover.

CYP2B1-3A4CT degradation in yeast: The differential sorting of mammalian ER-anchored CYPs 2B1, 2C11 and 3A4 into two distinct proteolytic pathways not only underscores the mechanistic diversity of the intracellular P450 degradation process, but also suggests that structural/molecular determinants may dictate the choice of degradation pathways. However, intrinsic determinants of such differential targeting have yet to be identified and could be located anywhere on the P450 protein. The P450 N-terminus is embedded in the ER membrane and this inaccessibility makes it *a priori* a considerably less plausible proteolytic targeting sequence than the cytosol-exposed P450 C-terminal domain (Yano et al., 2004; Williams et al., 2004). Thus as an initial approach to identifying structural features that commit P450s to either of these two pathways, we examined the potential role of the extreme C-terminus of the protein in the differential proteolytic targeting of P450s. For this purpose, the degradation of a chimeric protein (CYP2B1-3A4CT; Fig. 5), consisting of the full-length CYP2B1 with seven CYP3A4 C-terminal residues appended at its C-terminus, was examined in *PEP4* and *pep4Δ* yeast strains (Fig. 6). In contrast to the dramatic stabilization of unmodified CYP2B1 (Fig. 4), no corresponding stabilization of the chimeric CYP2B1-3A4CT protein was observed in the *pep4Δ* strain at the stationary growth stage (Fig. 6), thereby revealing that this CYP2B1 chimeric protein was no longer dependent on the vacuolar pathway for its degradation. Consistent with this apparent switch in the route of degradation, expression of the CYP2B1-3A4CT chimera in *hrd2-1* yeast led to a statistically significant two-fold stabilization of this protein (Fig. 7), while the unmodified CYP2B1 protein was unaffected in this yeast strain (Fig. 3). These findings thus

revealed that the incorporation of the CYP3A4 C-terminal heptapeptide was sufficient to target the chimeric CYP2B1-3A4CT protein for 26S proteasomal degradation in a manner similar to that of the wild type CYP3A4 protein. However, unlike the presumably coupled Ubc7p/Hrd2p-dependence of the degradation of native CYP3A4 protein, no corresponding Ubc7p dependence was found for CYP2B1-3A4CT as determined by the lack of appreciable stabilization of the chimeric protein after its expression in *ubc7Δ* yeast (Fig. 8). Thus, the proteasomal degradation of CYP2B1-3A4CT either involves ubiquitination by an Ub-conjugating enzyme other than Ubc7p, or is independent of ubiquitination, a less likely possibility given the Hrd2p (19S cap subunit)-dependent degradation of this modified CYP2B1 protein.

The possibility that the observed proteasomal degradation of CYP2B1-3A4CT is due to misfolding and consequent instability of the chimeric protein relative to that of the unmodified CYP2B1 was excluded by the following criteria: Each P450 protein was heterologously expressed in two different yeast strains and microsomal fractions prepared from cells harvested at the early growth stage of culture. The spectrally detectable microsomal P450 (holoenzyme) contents of CYP2B1-3A4CT and unmodified CYP2B1 (Fig. 9) were compared to their contents of immunodetectable CYP2B1 protein (Table 2). Comparable ratios of holoenzyme content/total CYP2B1-immunoreactive protein content indicated equivalent efficiencies of folding and hemoprotein assembly of both proteins in both yeast strains examined (Table 2). Furthermore, when these proteins were heterologously expressed in *E. coli*, a considerably higher yield of CYP2B1-3A4CT than that of the parent CYP2B1 was observed (Table 3), a finding inconsistent with a folding defect for this modified protein. Functional reconstitution of the partially purified heterologously expressed recombinant proteins using testosterone 16 β -hydroxylase as a CYP2B1-selective functional probe, also revealed comparable specific activities, thereby indicating no alteration in function by the CYP3A4CT modification (Table 3). Since both the P450 holoenzyme spectrum and the catalytic activity are sensitive measures of the integrity of

Mol #9654

the CYP2B1 protein, it appears that the altered degradation of CYP2B1-3A4CT compared to that of the unmodified CYP2B1 is not due to any structural change affecting the active site.

DISCUSSION

The finding that native CYP2B1 incurs Pep4p-dependent vacuolar degradation after its heterologous expression in *S. cerevisiae* (Fig. 4) establishes that its proteolytic course in yeast is analogous to its normal (lysosomal) route in the rat liver. Thus, in spite of being an “alien” protein, CYP2B1 is degraded via the yeast vacuolar pathway rather than by the Ub-dependent 26S proteasomal system, the pathway for degradation of abnormal proteins. These findings thus further validate *S. cerevisiae* as a reliable model for the characterization of hepatic CYP2B1 degradation. Together with our previous findings (Murray and Correia, 2001; Murray et al., 2002) they also confirm that in yeast, as in the mammalian liver, the longer-lived P450 proteins (CYPs 2B1 and 2C11) undergo vacuolar degradation whereas the shorter turnover proteins (CYPs 3A) undergo proteasomal degradation⁵. On the other hand, mammalian liver CYP2E1, which exhibits biphasic turnover with a rapid phase component of $t_{1/2} \approx 7$ h, and a slow phase component of $t_{1/2} \approx 37$ -38 h, apparently is a substrate of both proteolytic systems (Bardag-Gorce et al., 2002; Roberts et al. 1995; Ronis et al., 1989, 1991; Tierney et al., 1992; Yang and Cederbaum, 1996). The differential processing of the same P450 protein may be related to the occupancy of its active site. Accordingly, CYP2E1 complexation with a substrate ligand such as ethanol or acetone stabilizes the enzyme, thereby increasing its content and converting it into a longer-lived species with a monophasic turnover with $t_{1/2} \approx 37$ -38 h that is susceptible to autophagic-lysosomal sequestration. However, substrate decomplexation (e.g. by ethanol withdrawal) converts the CYP2E1 protein into a rapid turnover species that is susceptible to proteasome-inhibitor sensitive degradation (Bardag-Gorce et al., 2002). Collectively, these findings suggest that substrate complexation can determine the relative fraction and interconvertability of the short- and long-lived CYP2E1 species and thus dictate the enzyme’s relative susceptibility to either of the two proteolytic pathways. Similar substrate-induced protein stabilization is also observed after metabolic intermediate complexation of dexamethasone-inducible CYP3A23 by the quasi-irreversible, mechanism-based inactivator,

troleandomycin (TAO)⁶. TAO is known to dramatically extend the half-lives of CYP3A23 apoprotein and heme moieties from \approx 14 and 10 h to 63 and 73 h, respectively, with an attendant marked “induction” of CYP3A23 content (Watkins et al. 1986). Whether such TAO-complexation also switches the proteolytic susceptibility of CYP3A23 from predominantly proteasomal to lysosomal degradation remains to be determined. It is noteworthy however that, in the absence of substrates, both CYP2E1 and CYP3A23 are highly prone to oxidative uncoupling and consequent oxidative damage. Thus, not surprisingly, suppression of such oxidative uncoupling through disruption of their prosthetic heme reduction (Henderson et al., 2003; Zhukov and Ingelman-Sundberg, 1999) or quasi-irreversible complexation of the P450 heme (Watkins et al. 1986), protects the enzyme from oxidative damage and rapid proteolysis with consequent protein stabilization. Given this possibility, it is conceivable that similar complexation of CYP2B1 with a substrate-inducer molecule and/or its relative resistance to oxidative uncoupling also account(s) for its relatively long protein half-life and its predominant targeting to lysosomal degradation in the rat liver (Masaki et al., 1987; Ronis et al., 1991). However, the above findings that (i) in the absence of any exogenously added CYP2B1 substrate, CYP2B1 in *S. cerevisiae* maintained in minimal medium is similarly targeted to the vacuole, the yeast lysosomal equivalent; and (ii) grafting of just seven additional CYP3A4 C-terminal residues onto the CYP2B1 C-terminus switches its proteolytic targeting without detectably altering the CYP2B1 protein or active site structure and/or function (Fig. 9, Table 3), argue for the plausible existence of specific determinants that dictate the route of proteolytic degradation of the native P450 protein. The notion that CYP3A4 could contain a proteasomal determinant is consistent with the fact that in yeast as in the liver, CYP3A4 retains its 26S proteasomal susceptibility. This is so even though the protein is almost certainly largely in its native state when so expressed, as its redox function, and hence its potential for damage inflicted by oxidative uncoupling, is greatly attenuated in the absence of coexpressed P450 reductase.

The precise identity of such proteolytic determinants and/or the nature of the signals for the differential proteolytic sorting in normal P450 turnover remain to be defined. Such determinants could include degradation motifs (i.e. “degrons”) inherent to the P450 protein structure or acquired and/or unmasked as a result of protein modification associated with the P450 oxidative/catalytic function. Common posttranslational modifications that predispose intracellular proteins for proteolytic removal include Ub-conjugation, glutathione-protein mixed disulfide formation, His, Cys or Met oxidations, phosphorylation/dephosphorylation, deamidation and glycosylation (Correia, 2003, *and references therein*). Intrinsic structural features of target proteins required for their recognition by proteolytic systems include Lys or N-terminal residues for Ub-conjugation, PEST/PAGE sequences for kinases/calpains and other Ca⁺²-dependent proteases, “destruction boxes”, degradation motifs, “KK” motifs, C-terminal basic or acidic residues for ER degradation, as well as KFERQ, [G]YXXØ, [DE]XXXL[LI] and DXXLL consensus motifs for lysosomal sorting/autophagy (Bonifacino and Traub, 2003; Dice et al., 1990; Johnson et al., 1990; King et al., 1996; Rogers et al., 1996; Sokolik and Cohen, 1992).

We find it intriguing that inspection of the CYP2B1 protein sequence reveals the existence of a lysosomal sorting signal⁷ in the N-terminal region of the protein: a [DE]XXXL[LI] motif at D₄₇RGGLL₅₂, conveniently located between the predicted CYP2B1 ER-membrane anchor and cytosolic domain. No corresponding lysosomal sorting motif is present in CYP3A4, a proteasomally degraded P450 protein. Furthermore, similar sequence analysis of CYP2C11, another lysosomally degraded protein, indicated that although it contains no corresponding [DE]XXXL[LI] motif, it does carry a lysosomal sorting GYXXØ motif at G₇₉YEAV₈₃. The presence of such determinants may insure lysosomal degradation as a “default” route for the native P450s. Whether these inherent P450 structural motifs by themselves are sufficient as lysosomal sorting determinants, or require additional, yet to be identified, cellular sorting and/or

trafficking machinery for their lysosomal recognition remains to be elucidated. Nevertheless, the ability of the CYP3A4 C-terminal heptapeptide to confer proteasomal susceptibility upon CYP2B1, an otherwise stable protein that is normally degraded by the lysosomes, suggests that such lysosomal determinants can be either overridden or suppressed. However, the documentation of Ub-dependent proteasomal degradation of the cumene hydroperoxide-inactivated CYP2B1 *in vitro* (Korsmeyer et al., 1999), reveals that the enzyme also harbors ubiquitination/proteasomal determinants that can be unmasked by its structural and functional inactivation.

The precise significance of the CYP3A4 C-terminus (D₄₉₇GTVSGA₅₀₃) as a potential proteasomal targeting determinant is presently unclear. The recently reported crystal structures of CYP3A4 reveal that this region is unstructured and entirely dispensable for correct folding⁸ (Williams et al., 2004; Yano et al., 2004). Thus, it is conceivable that this unstructured CYP3A4 region serves as a recognition signal for degradation by engaging either a 19S cap subunit before protein unfolding and/or insertion into the proteasomal catalytic barrel, or a yet to be identified Ub-ligase that ubiquitinates the protein before its delivery to the 26S proteasome (Pickart and Cohen, 2004). It is intriguing in this context, that the proteasomal targeting and subsequent proteolytic processing of ornithine decarboxylase (ODC), a 461 residue long protein, is also dependent on a flexible, unstructured 37-residue C-terminal region as a recognition signal (Zhang et al., 2003, 2004). Cys₄₄₁ and the extreme C-terminal pentapeptide (A₄₅₇RINV₄₆₁) in this ODC region are apparently indispensable for its insertion into the proteasomal catalytic chamber before its degradation. Furthermore, this 37-amino acid C-terminal tail can function as a proteasomal targeting signal when appended to other proteins (Zhang et al., 2003). The possibility of the CYP3A4 C-terminal heptapeptide similarly functioning as a degron is particularly compelling not only because it conferred proteasomal susceptibility on CYP2B1 but also because, as discussed above, it may enable CYP3A4 in spite

of its functional sluggishness in yeast, to retain its preferential degradation by the proteasome. Studies are currently underway to determine (i) which, if any, of the CYP3A4 heptapeptide (D₄₉₇GTVSGA₅₀₃) residues are essential for a functional proteasomal degnon, (ii) if this appendage could similarly switch the targeting of another *bona fide* lysosomal substrate, (iii) whether its excision from the CYP3A4 C-terminus would stabilize the enzyme by rendering it non-susceptible to proteasomal degradation and (iv) whether it could be replaced by any other similarly unstructured peptide.

In summary, the results described above indicate that as in the rat liver, the vacuolar pathway is responsible for the degradation of CYP2B1 in *S. cerevisiae*, thereby validating this model for the characterization of mammalian liver P450 degradation. Furthermore, these findings also indicate that the proteolytic susceptibility of CYP2B1 can be switched from predominantly lysosomal to proteasomal degradation merely by appending seven CYP3A4 C-terminal residues, thereby suggesting that this CYP3A4 region could serve as a proteasomal degnon.

ACKNOWLEDGEMENTS:

The authors wish to gratefully thank Prof. Randy Hampton, UCSD, for the generous gift of the yeast strains, Prof. James R. Halpert (UT, Galveston) for the gift of the plasmids pSW1 (encoding intact CYP2B1) and pKKCYP2B1(His)₄, and Prof. Eric F. Johnson, Scripps Institute, La Jolla, for providing pertinent CYP3A4 structural information before its publication. We thank Dr. Ping Kang for his generous assistance with the P450 purification and functional reconstitution studies. We also acknowledge the many publications that could not be cited due to the stipulated limit to the number of literature citations.

REFERENCES

- Bardag-Gorce F, Li J, French BA, and French SW (2002) Ethanol withdrawal induced CYP2E1 degradation in vivo blocked by proteasome inhibitor PS-341. *Free Rad Biol Med.* 32: 17-21
- Benharouga M, Haardt M, Kartner N and Lukacs G (2001). COOH-terminal truncations promote proteasome-dependent degradation of mature cystic fibrosis transmembrane conductance regulator from post-Golgi compartments. *J. Cell Biol.* 153:957-970.
- Bonifacino JS and Traub LM (2003) Signals for sorting of transmembrane proteins to endosomes and lysosomes. *Annu Rev Biochem.* 72:395-447.
- Correia MA (1991). Cytochrome P450 turnover. *Methods Enzymol.* 206:315-325
- Correia MA (2003) Hepatic cytochrome P450 degradation: Mechanistic diversity of the cellular sanitation brigade. *Drug Metab Rev.* 35:107-143
- Dice JF, Terlecky SR, Chiang HL, Olson TS, Isenman LD, Short-Russell SR, Freundlieb S, and Terlecky LJ. (1990) A selective pathway for degradation of cytosolic proteins by lysosomes. *Semin Cell Biol.* 1:449-455.
- Hampton RY, Gardner RG and Rine J (1996) Role of 26S proteasome and *HRD* genes in the degradation of 3-hydroxy-3-methylglutaryl-CoA reductase, an integral endoplasmic reticulum membrane protein. *Mol. Biol. Cell* 7:2029-2044.
- Hampton RY. (2002a) ER-associated degradation in protein quality control and cellular regulation. *Curr Opin Cell Biol.*14:476-482.
- Hampton RY. (2002b) Proteolysis and sterol regulation. *Annu Rev Cell Dev Biol.* 18:345-378.
- He, K, Falick, AM, Chen, B, Nilsson, F and Correia, MA (1996): Identification of the heme-adduct and an active site peptide modified during mechanism-based inactivation of rat liver cytochrome P450 2B1 by secobarbital. *Chem Res Tox* 9:614-622.

- Henderson CJ, Otto DM, Carrie D, Magnuson MA, McLaren AW, Rosewell I, and Wolf CR. (2003) Inactivation of the hepatic cytochrome P450 system by conditional deletion of hepatic cytochrome P450 reductase. *J Biol Chem.* 278:13480-13486.
- Huan J-Y, Streicher JM, Bleye LA, and Koop DR. (2004). Proteasome-dependent degradation of cytochromes P450 2E1 and 2B1 expressed in tetracycline-regulated HeLa cells. *Tox. Appl. Pharmacol.* 199:332-343.
- John GH, Hasler JA, He YA, and Halpert JR. (1994) *Escherichia coli* expression and characterization of cytochromes P450 2B11, 2B1, and 2B5. *Arch Biochem Biophys.* 314:367-375.
- Johnson P, Swanson R, Rakhilina L and Hochstrasser, M. (1998). Degradation signal masking by heterodimerization of MATalpha2 and MATa1 blocks their mutual destruction by the ubiquitin-proteasome pathway. *Cell* 94:217-227.
- King R, Glotzer M. and Kirschner, M. (1996). Mutagenic analysis of the destruction signal of mitotic cyclins and structural characterization of ubiquitinated intermediates. *Mol Biol Cell* 7:1343-1357
- Kornitzer D. (2002) Monitoring protein degradation *Methods Enzymol.* 351: 639-647.
- Korsmeyer KK, Davoll S, Figueiredo-Pereira ME, and Correia MA. (1999) Proteolytic degradation of heme-modified hepatic cytochromes P450: A role for phosphorylation, ubiquitination, and the 26S proteasome? *Arch Biochem Biophys.* 365:31-44.
- Kostova Z and Wolf DH. (2003) For whom the bell tolls: protein quality control of the endoplasmic reticulum and the ubiquitin-proteasome connection. *EMBO J.* 22:2309-2317.
- Meyer H, Shorter J, Seemann J, Pappin D, and Warren G. (2000) A complex of mammalian ufd1 and npl4 links the AAA-ATPase, p97, to ubiquitin and nuclear transport pathways. *EMBO J.* 19:2181-2192

- Murray BP, and Correia MA. (2001) Ubiquitin-dependent 26 S proteasomal pathway: A role in the degradation of the native human liver CYP3A4 expressed in *Saccharomyces cerevisiae*? *Arch Biochem Biophys.* 393:106-116
- Murray BP, Zgoda VG, and Correia MA. (2002) Native CYP2C11: Heterologous expression in *Saccharomyces cerevisiae* reveals a role for vacuolar proteases rather than the ubiquitin-26S proteasome system in the degradation of this endoplasmic reticulum enzyme. *Mol Pharmacol.* 61:1146-1153
- Masaki R, Yamamoto A. and Tashiro Y. (1987). Cytochrome P-450 and NADPH-cytochrome P-450 reductase are degraded in the autolysosomes in rat liver. *J Cell Biol.* 104:1207-1215.
- Pickart CM and Cohen RE. 2004. Proteasomes and their kin: proteases in the machine age. *Nat Rev Mol Cell Biol.* 5:177-187
- Roberts BJ, Song BJ, Soh Y, Park SS and Shoaf SE. (1995). Ethanol induces CYP2E1 by protein stabilization. Role of ubiquitin conjugation in the rapid degradation of CYP2E1. *J Biol Chem.* 270:29632-29635.
- Rogers S, Wells R and Rechsteiner M. (1986). Amino acid sequences common to rapidly degraded proteins: the PEST hypothesis. *Science* 234:364-368.
- Ronis MJ and Ingelman-Sundberg, M. (1989). Acetone-dependent regulation of cytochrome P-450j (IIE1) and P-450b (IIB1) in rat liver. *Xenobiotica* 19:1161-1165.
- Ronis MJ, Johansson I, Hultenby K, Lagercrantz J, Glaumann H and Ingelman-Sundberg M. (1991). Acetone-regulated synthesis and degradation of cytochrome P450E1 and cytochrome P450B1 in rat liver. *Eur J Biochem.* 198:383-389.
- Sokolik CW and Cohen RE. (1992). Ubiquitin conjugation to cytochromes c. Structure of the yeast ISO-1 conjugate and possible recognition determinants. *J Biol Chem.* 267:1067-1071

- Song BJ, Veech RL, Park SS, Gelboin HV and Gonzalez FJ. (1989). Induction of rat hepatic N-nitrosodimethylamine demethylase by acetone is due to protein stabilization. *J Biol Chem.* 264:3568-3572.
- Roberts BJ. Evidence of proteasome-mediated cytochrome P-450 degradation. (1997) *J Biol Chem.*, 272: 9771-9778.
- Tierney DJ, Haas AL and Koop DR. (1992) Degradation of cytochrome P450 2E1: Selective loss after labilization of the enzyme. *Arch. Biochem. Biophys.* 29: 9-16.
- Wang H, Dick R, Yin H, Licad-Coles E, Kroetz D, Szklarz G, Halpert J R and Correia M.A. (1998) Structure-function relationships of human liver cytochromes P450 3A: Aflatoxin B1 metabolism as a probe. *Biochemistry* 37: 12536-12545.
- Watkins PB, Wrighton SA, Schuetz EG, Maurel P and Guzelian PS. (1986). Macrolide antibiotics inhibit the degradation of the glucocorticoid-responsive cytochrome P-450p in rat hepatocytes in vivo and in primary monolayer culture. *J Biol Chem.* 261:6264-6271.
- Watkins PB, Bond JS and Guzelian PS. (1987). Degradation of the hepatic cytochromes P-450. in *Mammalian Cytochromes P450*. (Guengerich, F.P., ed.) Vol. II, pp. 173-192, CRC Press, Inc., Boca Raton, FL.
- Wilhovsky S, Gardner R, and Hampton R. (2000). HRD gene dependence of endoplasmic reticulum-associated degradation. *Mol Biol Cell* 11:1697-1708
- Williams PA, Cosme J, Vinkovic DM, Ward A, Angove HC, Day PJ, Vonrhein C, Tickle IJ, and Jhoti H. (2004) Crystal structures of human cytochrome P450 3A4 bound to metyrapone and progesterone. *Science.* 305:683-686.
- Wolf DH. (2004) From lysosome to proteasome: the power of yeast in the dissection of proteinase function in cellular regulation and waste disposal. *Cell Mol Life Sci.* 61:1601-1614.
- Yang MX and Cederbaum A.I. (1996) Role of the proteasome complex in degradation of human CYP2E1 in transfected HepG2 cells. *Biochem Biophys Res Commun.* 226: 711-716.

- Yano JK, Wester MR, Schoch GA, Griffin KJ, Stout CD, and Johnson EF. (2004) The Structure of Human Microsomal Cytochrome P450 3A4 Determined by X-ray Crystallography to 2.05 Å Resolution. *J Biol Chem.* 279:38091-38104.
- Zhang M, Pickart CM, and Coffino P. (2003) Determinants of proteasome recognition of ornithine decarboxylase, a ubiquitin-independent substrate. *EMBO J.* 22:1488-1496.
- Zhang M, MacDonald AI, Hoyt MA, and Coffino P. (2004) Proteasomes begin ornithine decarboxylase digestion at the C terminus. *J Biol Chem.* 279:20959-20965.
- Zhukov A and Ingelman-Sundberg M. (1999) Relationship between cytochrome P450 catalytic cycling and stability: fast degradation of ethanol-inducible cytochrome P450 2E1 (CYP2E1) in hepatoma cells is abolished by inactivation of its electron donor NADPH-cytochrome P450 reductase. *Biochem J.* 340: 453-8.

FOOTNOTES

These studies were supported by NIH grants GM44037 and DK26506. We also acknowledge the UCSF Liver Core Center Facility (Molecular Analyses/Spectrophotometry) supported by P30DK26743.

1. Present Address: Institute of Biomedical Chemistry, Russian Academy of Medical Sciences, R-119992 Moscow, Russia.
2. Present address: Drug Metabolism Department, Abbott Laboratories, Abbott Park, IL 60064.
3. Individual liver microsomal P450s turn over asynchronously, with the heme turnover being relatively more rapid and constant ($t_{1/2} \approx 8-10$ h) than that of the protein moiety ($t_{1/2} \approx 7-37$ h) (Correia, 1991, *and references therein*).
4. This was established for CYP2B1 by quantitative immunoblotting analyses coupled with ferritin-immunoelectron microscopy in PB/leupeptin-pretreated rats (Masaki et al., 1987) and for CYPs 2B1 and E1 by quantitative immunoblotting analyses in acetone/leupeptin-pretreated rats (Ronis et al., 1991) and cultured rat hepatocytes (Roberts et al., 1995). Note that as discussed (Discussion) native rat liver CYP2E1 turns over biphasically in vivo with a short half-life of ≈ 7 h and a longer half-life of ≥ 37 h, depending on its active site substrate complexation (Bardag-Gorce et al., 2002; Roberts et al., 1995; Song et al., 1989).
5. This raises the issue of intracellular “protein trafficking” which undoubtedly must occur during P450 degradation as the ER-anchored proteins are extracted from the ER membrane and translocated either to the vacuoles or the proteasome in the cytosol, or even, albeit minutely, to the cell membrane. As explained above, from the design of the experiment with qualitative pairwise comparisons of mutant strain *versus* isogenic wild

type, we believe that our general qualitative conclusions of vacuolar *versus* proteasomal routes of degradation remain valid even if there are changes in trafficking. Thus, if the hrd2-1 defect (known to inactivate the proteasome) has no effect on CYP2B1 stability while deletion of pep4p (known to inactivate the vacuole albeit indirectly, through impairment of vacuolar protease maturation) stabilises the protein then the logical conclusion is that the degradation of CYP2B1 is dependent upon the vacuole (even if only indirectly). We believe that the same argument could apply to potential changes in protein trafficking.

6. TAO-mediated CYP3A mechanism-based inactivation is “quasi-irreversible” in that the enzyme can be catalytically reactivated by ferricyanide induced heme-iron oxidation which dissociates the TAO-nitrene:CYP3A complex, thereby regenerating the enzyme.
7. The dileucine [DE]XXXL[LI] lysosomal sorting signal requires an acidic residue at position -4, from the first invariant Leu of the LL/LI peptide motif, with three random residues (XXX) at intervening positions. A bona fide YXXØ lysosomal sorting motif usually contains a Gly residue preceding the invariant Tyr residue, two random residues (XX) followed by a bulky hydrophobic side chain (Ø) residue at +3 (Bonifacino and Traub, 2003).
8. By contrast, C-terminal truncation of ER-proteins such as the mature cystic fibrosis transmembrane conductance regulator (CFTR) (Benharouga et al., 2001) and CYP2E1 (Huan Y-J et al., 2004) accelerates their proteasomal degradation through increased structural instability of the proteins.

FIGURE LEGENDS:

Fig. 1. The cellular ERAD and vacuolar proteolytic machinery of *S. cerevisiae*. The ER-bound polytopic Hmg2p and the monotopic P450s (2B1, 2B1-3A4CT, 3A4 and 2C11) are illustrated schematically. With the exception of Ubc6p, all the other proteins (Ubc7p, Cue1p, Hrd1p/Hrd3p and Hrd2p) have been shown to be required for the *UBC/HRD*-dependent ERAD of the integral protein Hmg2p (*shown*) or luminal protein CPY* (*not shown*) (Hampton 2000a, 2000b; Kostova and Wolf, 2003). Ubc7p and Hrd2p are also required for CYP3A4 ERAD in yeast. The yeast vacuolar *PEP4*-dependent system is also shown. The solid arrows indicate the major pathways for the degradation of particular P450 proteins. See the text for details.

Fig. 2. Relative degradation of rat CYP2B1 in wt and *ubc*-deficient *S. cerevisiae* strains. Yeast strains transformed with the CYP2B1 expression vector (pYcDE/2B1) or the empty vector (pYcDE-2; *not shown*) were grown at 30°C in SD with appropriate supplements. Cells were harvested at an early culture stage during logarithmic growth phase (\approx OD of 1.0 at 600 nm), or at a late stage after "stationary chase" (generally, 20 to 24 h after reaching an OD at 600 nm of 0.5). Microsomal protein prepared from these cells was subjected to western immunoblotting analyses with anti-CYP2B1 IgGs. A representative immunoblot from one of the three experiments is included. The relative densitometric quantitation of immunoblots at the late stages of culture is expressed as per cent of the corresponding values (100%) at the early stage. Values represent the mean \pm SD of at the least three individual experiments. No statistically significant differences were found between these values.

Fig. 3. Relative degradation of rat CYP2B1 in wt and *hrd*-mutant *S. cerevisiae* strains. For experimental details see Fig. 2. Values represent the mean \pm SD of at the least three individual experiments, with no statistically significant differences found between them.

Fig. 4. Relative stabilization of rat CYP2B1 in PEP4 and pep4Δ S. cerevisiae strains. For experimental details see Fig. 2. Values represent the mean ± SD of at the least three individual experiments. The asterisk indicates a statistically significant ($p < 0.01$) difference in expression relative to the corresponding wt control.

Fig. 5. The chimeric CYP2B1-3A4CT construct. The N-terminally anchored CYPs 2B1, 3A4, and 2B1-3A4CT in the ER-bilayer are schematically depicted (*top*). N and C refer to the P450 extreme N- and C-termini, respectively. The C-terminal amino acid sequence of each P450 beyond residue 484 is shown in its entirety (*below*). The chimeric CYP2B1-3A4CT protein consists of the extreme CYP3A4 C-terminal D₄₉₇GTVSGA₅₀₃ peptide grafted onto the CYP2B1 C-terminus. For details see Materials and Methods.

Fig. 6. Relative stabilization of CYP2B1-3A4CT in wt (PEP4) and pep4Δ S. cerevisiae strains. The expression plasmid used was pYES2-ADH/CYP2B1-3A4CT. For other experimental details see Fig. 2. Values represent the mean ± SD of at the least three individual experiments, with no statistically significant difference found between them.

Fig. 7. Relative stabilization of rat CYP2B1-3A4CT in wt and hrd2-1 mutant S. cerevisiae strains. For experimental details see Fig. 2. Values each represent the mean ± SD of at the least three individual experiments. The asterisk indicates a statistically significant difference at $p < 0.05$ relative to the corresponding wt control.

Fig. 8. Relative degradation of CYP2B1-3A4CT in wt and ubc7-deficient S. cerevisiae strains. For experimental details see Fig. 2. Values represent the mean ± SD of at the least

three individual experiments, with no statistically significant difference found between them.

Fig. 9. Spectrally detected microsomal P450 content. Yeast strain RHY718 (wt, *HRD*) transformed with either expression plasmid (1) pYcDE/2B1 (CYP2B1) or (2) pYcDE/2B1-3A4CT (CYP2B1-3A4CT) was grown at 30°C in SD with appropriate supplements. Cells were harvested during logarithmic growth phase (early stage), and the reduced CO-difference spectra of yeast microsomal CYP2B1 and CYP2B1-3A4CT preparations (2 mg protein/mL) determined as described previously (Murray et al., 2001).

Table 1. Yeast strains used in our studies

Strains	Genotype
RHY718 (<i>wt, HRD</i>)	<i>MATα ade2-101 met2 his3Δ200 hmg2::HIS3 lys2-801 hmg1::LYS2 leu2Δ trp1Δ ura3-52 +pRH244 (URA3, 6mycHMG2)</i>
RHY609 (<i>hrd1Δ</i>)	<i>MATα ade2-101 met2 his3Δ200 hmg2::HIS3 lys2-801 hmg1::LYS2 LEU trp1::hisG ura3-52::6mycHMG2 hrd::URA3</i>
RHY925 (<i>hrd2-1</i>)	<i>MATα ade2-101 met2 his3Δ200 hmg2::HIS3 lys2-801 hmg1::LYS2 leu2Δ trp1Δ URA3::6MycHMG2 hrd2-1</i>
RHY749 (<i>hrd3Δ</i>)	<i>MATα ade2-101 met2 his3Δ200 hmg2::HIS3 lys2-801 hmg1::LYS2 leu2Δ trp1Δ ura3-52::6MycHMG2 hrd3::URA3</i>
RHY1166 (<i>wt, UBC</i>)	<i>MATα ade2-101 met2 his3Δ200 hmg2::HIS3 lys2-801 hmg1::LYS2 leu2Δ trp1Δ ura3-52::MycHMG2</i>
RHY1596 (<i>ubc6Δ</i>)	<i>MATα ade2-101 met2 his3Δ200 hmg2::HIS3 lys2-801 hmg1::LYS2 leu2Δ trp1Δ ura3-52::MycHMG2 ubc6::KanMX</i>
RHY1603 (<i>ubc7Δ</i>)	<i>MATα ade2-101 met2 his3Δ200 hmg2Δ-4 lys2-801 hmg1::LYS2 leu2Δ trp1Δ ura3-52::MycHMG2 ubc7::HIS3</i>
RHY1604 (<i>ubc6Δ/7Δ</i>)	<i>MATα ade2-101 met2 his3Δ200 hmg2Δ-4 lys2-801 hmg1::LYS2 leu2Δ trp1Δ ura3-52::MycHMG2 ubc6::KanMX ubc7::HIS3</i>
RHY473 (<i>wt, PEP4</i>)	<i>ade2-101 met2 his3Δ200 lys2-801 ura3-52</i>
RHY106-4 (<i>pep4Δ</i>)	<i>ade2-101 met2 his3Δ200 lys2-801 ura3-52 pep4Δ</i>

Table 2: The ratios of microsomal CYP2B1 and CYP2B1-3A4CT holohemoprotein and total CYP2B1 immunoreactive protein expressed in *S. cerevisiae*.

Yeast strain ^a	P450 ^b	Total CYP2B protein ^c (pmol/mg)	P450 Content ^d (pmol/mg)	Ratio ^e
RHY718	CYP2B1	27 ± 5	18 ± 9	0.76 ± 0.15
RHY718	CYP2B1-3A4CT	30 ± 10	22 ± 10	0.70 ± 0.12
RHY473	CYP2B1	12 ± 1	8 ± 2	0.66 ± 0.11
RHY473	CYP2B1-3A4CT	15 ± 1	10 ± 4	0.68 ± 0.25

^a The genotypes of the yeast strains used are described in Table 1. Yeast were grown in three separate 2L-batches and harvested at the early logarithmic growth stage (see Materials and Methods for details).

^b The yeast strain RHY 718 was transformed with the expression plasmid pYcDE/2B1 (CYP2B1) or pYcDE/2B1-3A4CT (CYP2B1-3A4CT), whereas the yeast strain RHY 473 was transformed with plasmid pYES2/2B1 (CYP2B1) or pYES2-ADH/2B1-3A4CT (CYP2B1-3A4CT) as described in Materials and Methods.

^c Microsomes were prepared and subjected to western immunoblotting analyses as described previously (Murray et al., 2001), with a purified liver CYP2B1 preparation used as the standard for quantitation.

^d The P450 spectral content was determined as described previously (Murray et al., 2001).

^e The molar ratio of P450 holocytochrome content/total CYP2B1 immunoreactive protein content is shown.

Table 3: The relative expression yields and functional activities of CYP2B1 and CYP2B1-3A4CT in *E. coli* DH5 α .

	P450 Yield (nmol/L)				Testosterone (T) 16 β -Hydroxylase Activity (nmol OH-T formed/nmol P450/min)	
	Harvest Time (h):	18	24	40		48
CYP2B1		49.4	130.7	120.8	32.8	3.6 \pm 0.5
CYP2B1-3A4CT		103.2	479	241.6		4.1 \pm 0.4

P450s were expressed in *E. coli* DH5 α cells as described (Materials and Methods). At the indicated times after induction, their total cellular P450 spectral content was monitored as described (Wang et al., 1998). P450 proteins from cells harvested at 40 h were partially purified, functionally reconstituted and their specific testosterone 16 β -hydroxylase activities determined in triplicate as described previously (He et al., 1996)

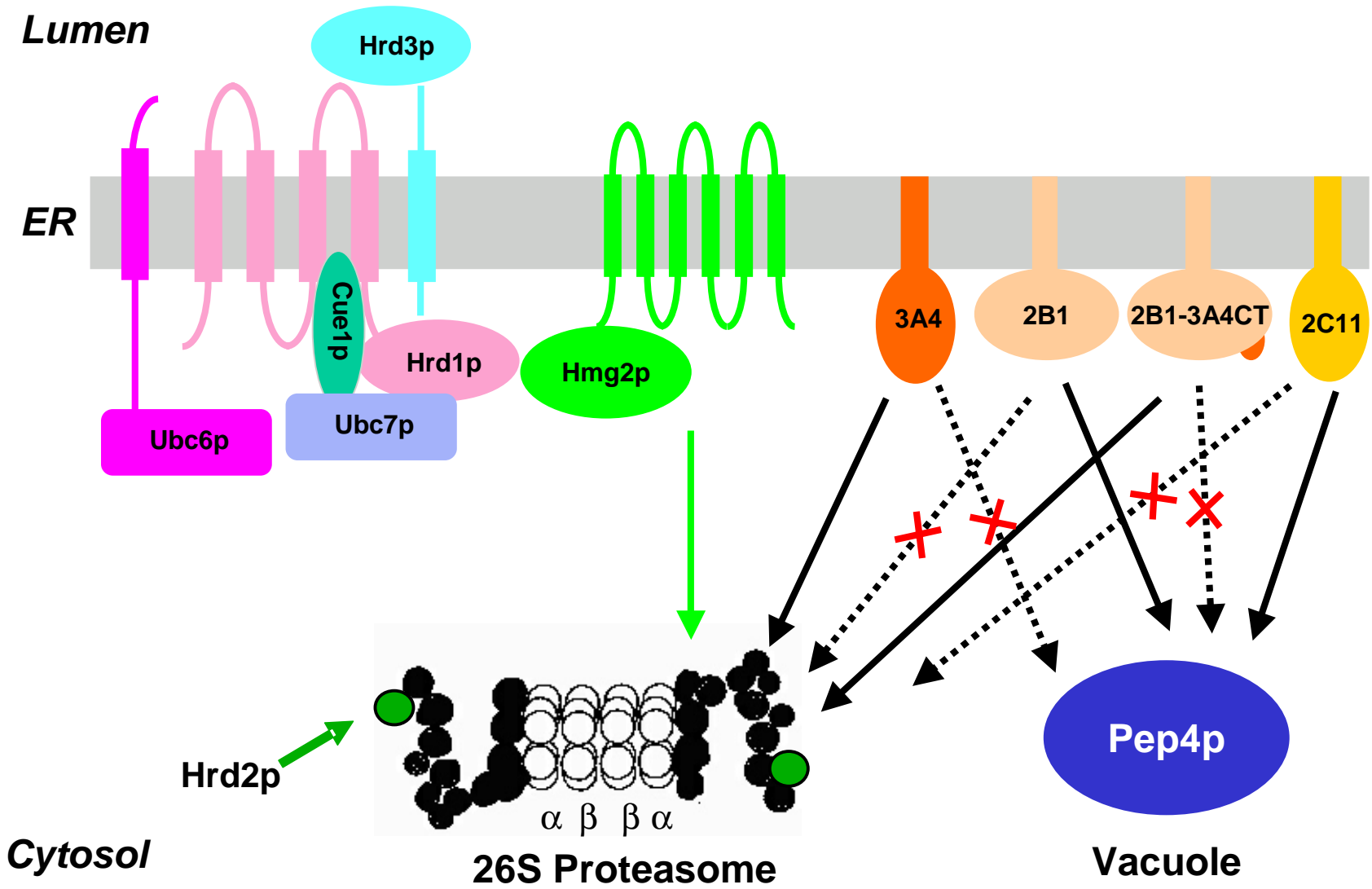


Figure 1

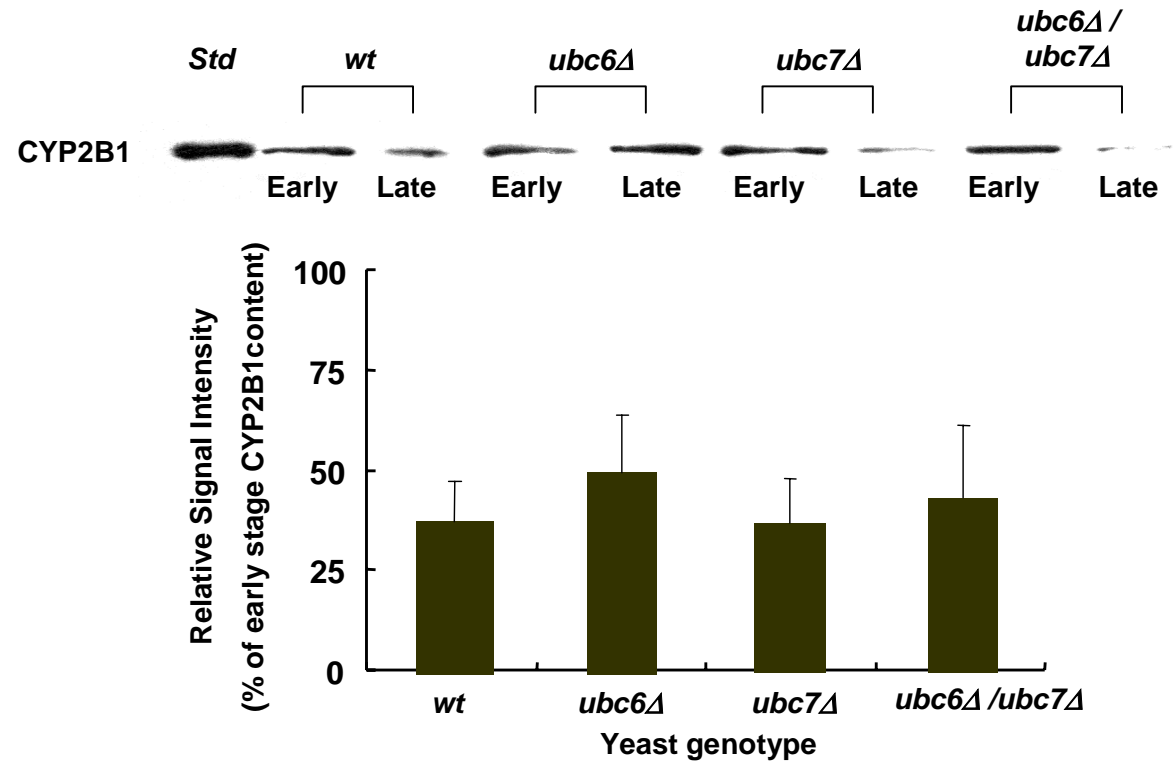


Figure 2

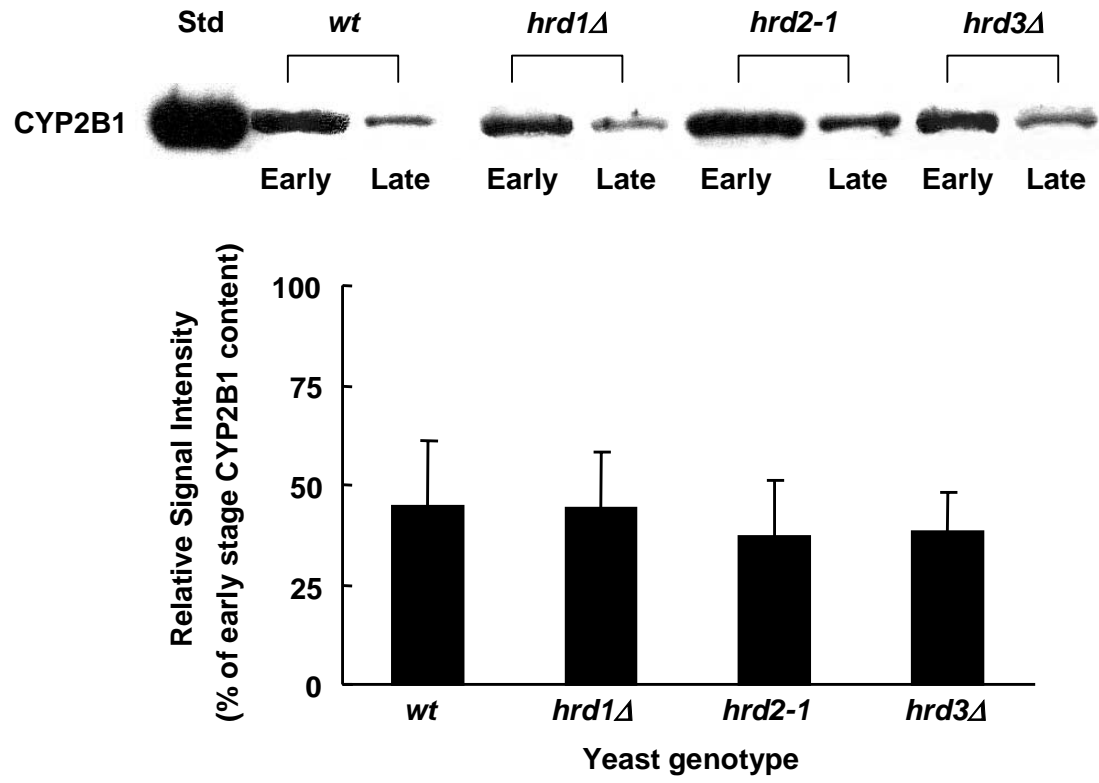


Figure 3

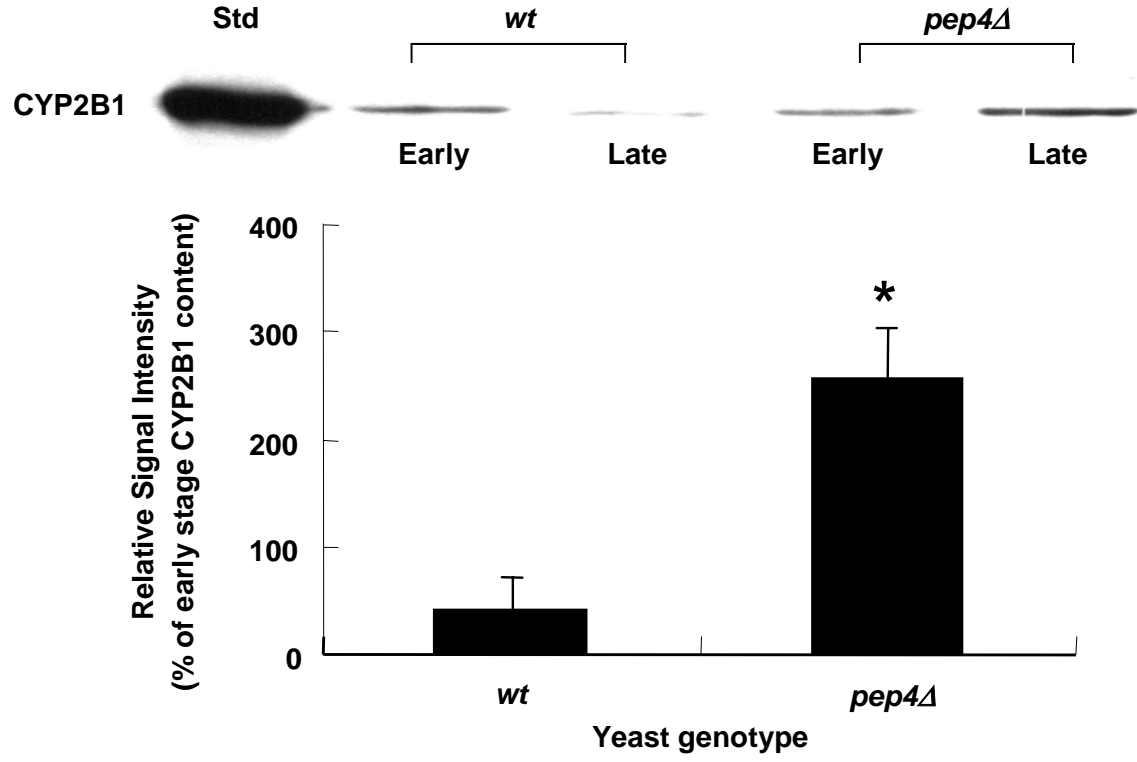
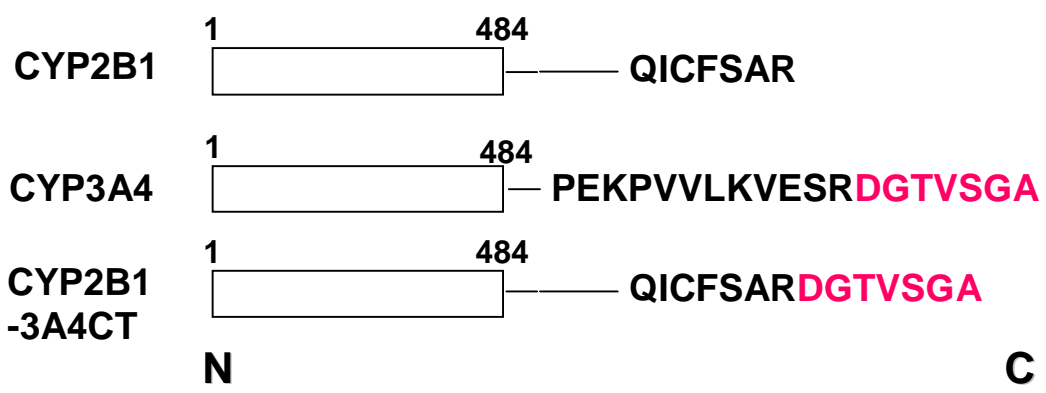
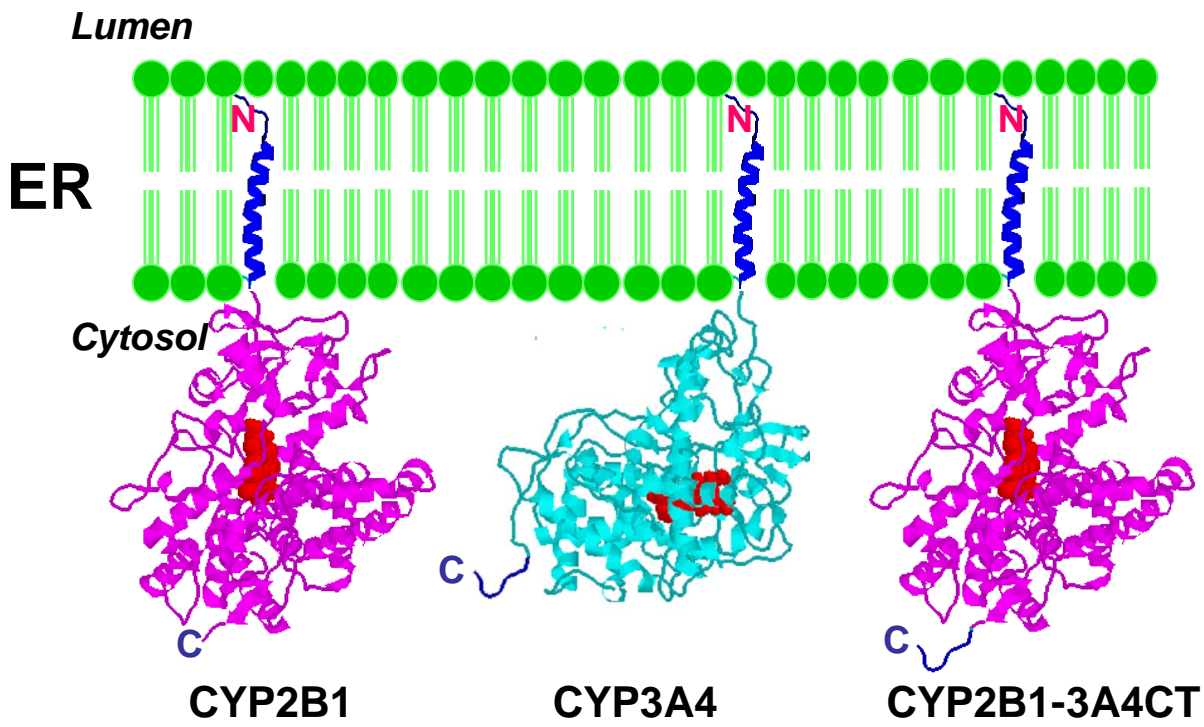


Figure 4



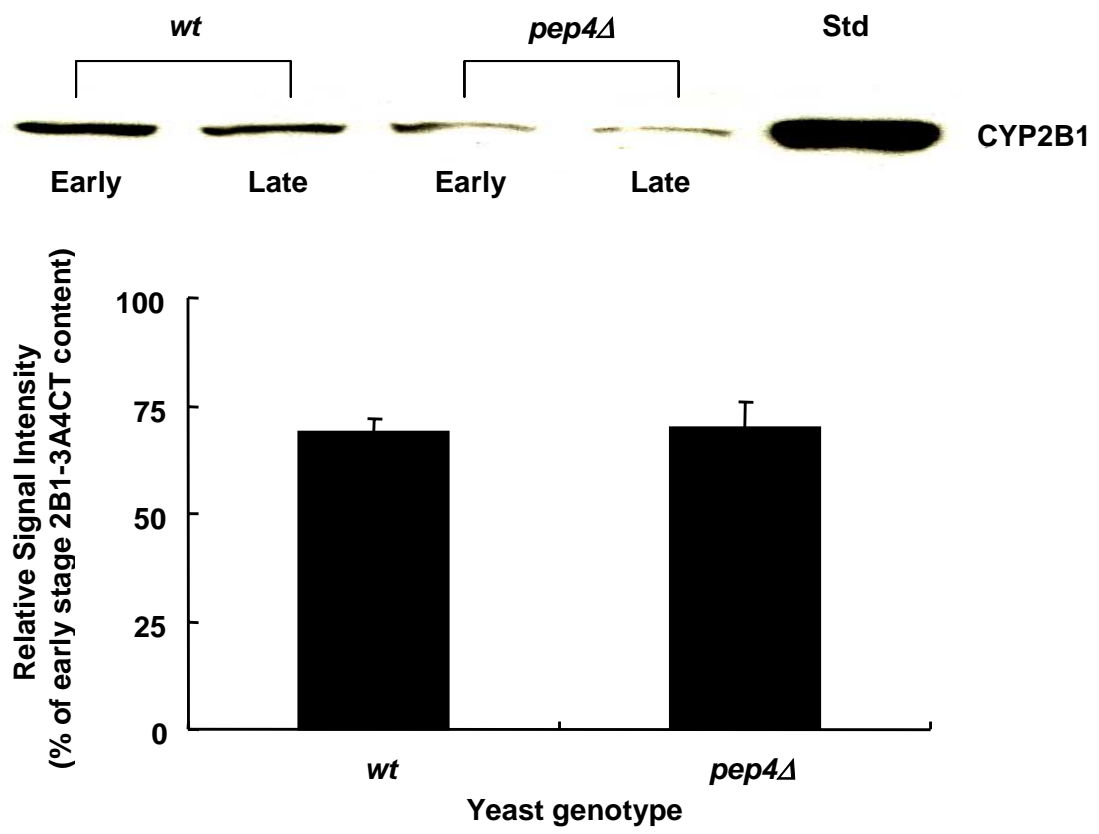


Figure 6

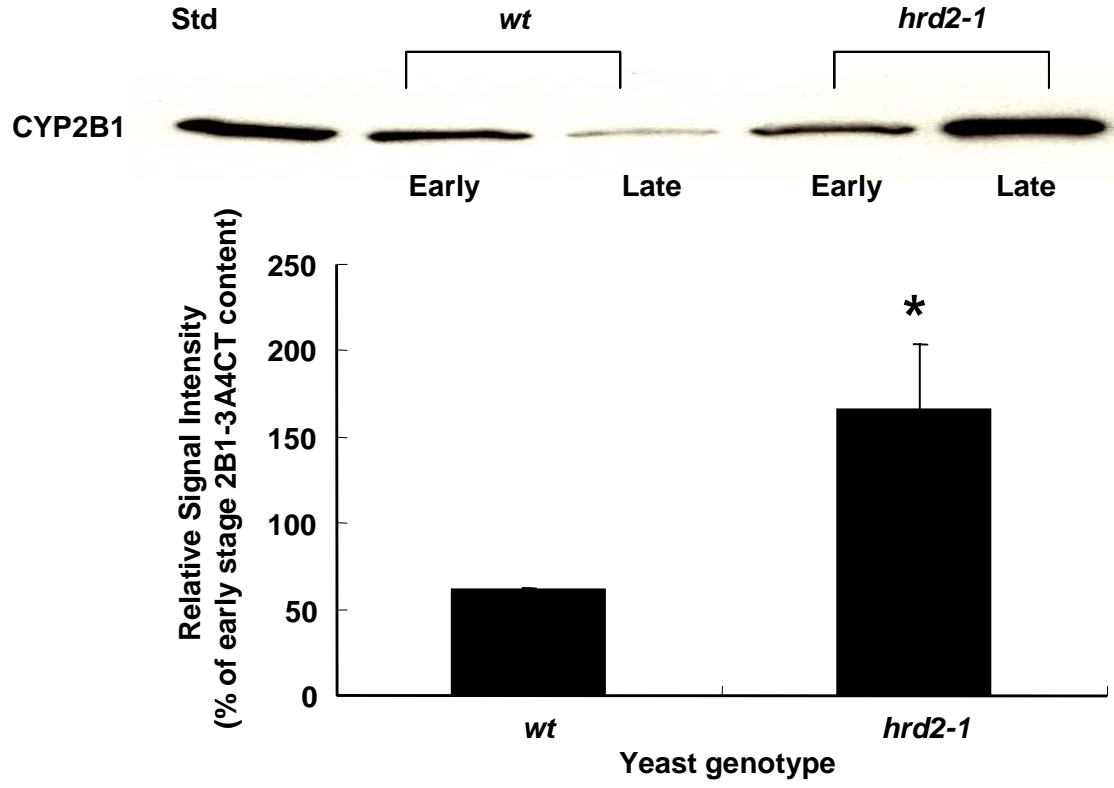


Figure 7

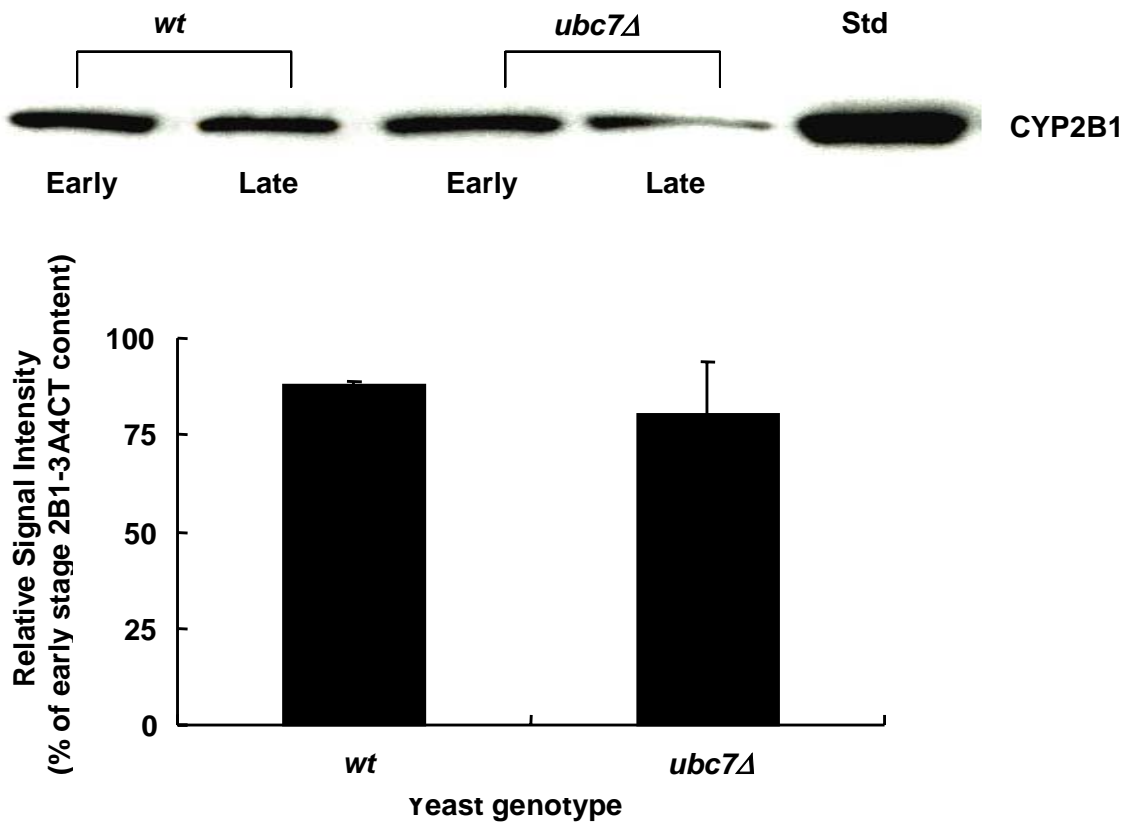


Figure 8

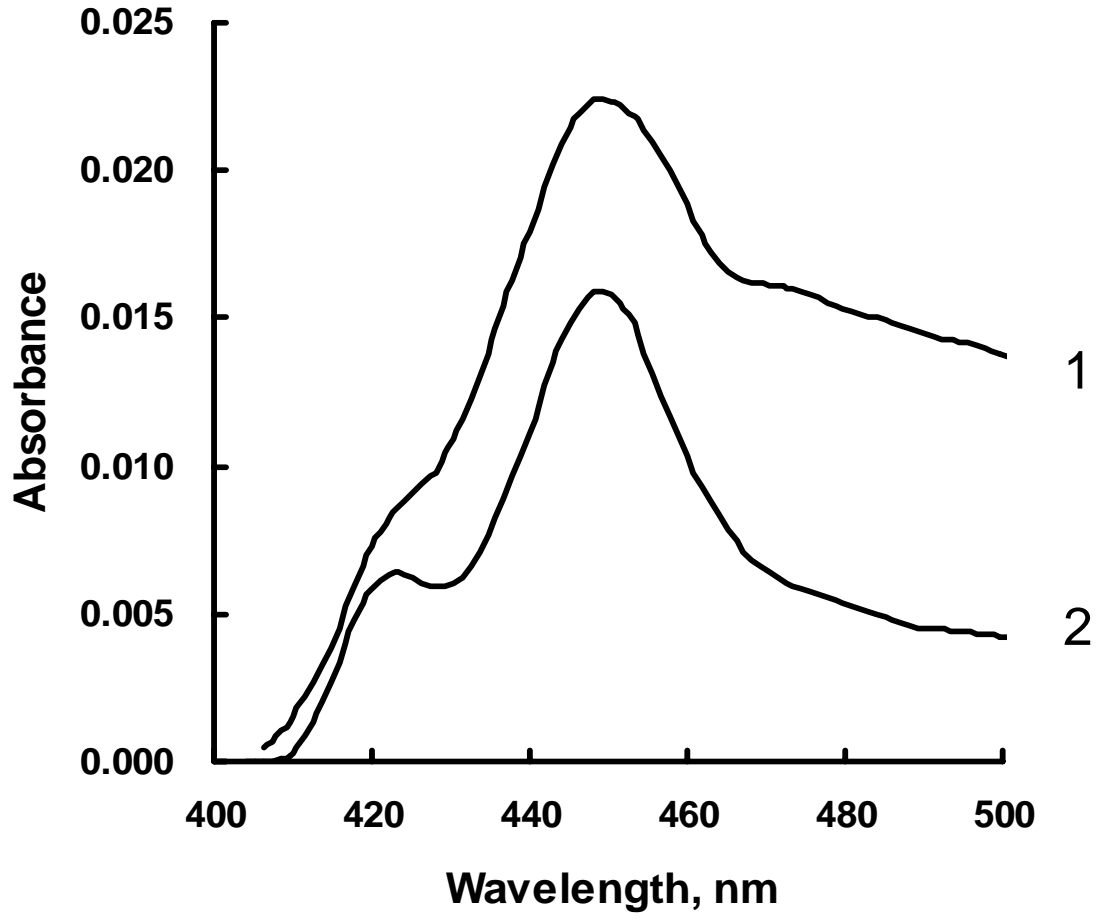


Figure 9